Pure & Appl. Chem., Vol. 60, No. 10, pp. 1517–1528, 1988.
Printed in Great Britain.

Colloidal metals: past, present and future

John M. Thomas

Davy Faraday Research Laboratory, The Royal Institution,
21, Albemarle Street, London, W1X 4BS, England

Abstract - A critical assessment of the various X-ray and electron-based methods of determining the structure of ultrafine metallic particles of colloidal dimension is given. In particular, examples of the use and potential of high-resolution electron microscopy of high-angle Rutherford scattering and of scanning tunneling microscopic procedures are illustrated. Several growth points of current and possible future uses of colloidal metals are identified; and the role of a variety of colloidal metals in (gas-solid) catalysis, in photocatalysis and in the photo-generation of organic materials are discussed. The prospects of fine-tuning colloidal catalysts are also briefly touched upon.

THE PAST

Colloidal metals are of ancient lineage. Several methods of preparing them were evolved well over a hundred years ago by Selmi, Faraday and Graham. They were the subject of lively studies by these and other pioneers including Tyndall, Rayleigh, Ostwald, Mie and Bredig and more recently by Rideal, who was among the first to probe their catalytic properties for selective conversions such as the hydrogenation of organic molecules. In numerous other respects, colloidal metals have played a prominent part in man's broader cultural activities: they figure eminently in stained glass windows and other decorative-artistic features, as well as in alchemical and medicinal contexts. In medieval times colloidal dispersions of gold, for example, were reputed to possess remarkable curative properties.

Faraday (ref. 1) prepared colloidal dispersions of gold by reducing an aqueous solution of a gold salt, such as sodium chloroaurate, with a solution of phosphorous in carbon disulphide. The reduction proceeds rapidly at room temperature and the bright yellow colour of the chloroaurate is replaced by the ruby colouration characteristic of colloidal gold (of appropriate average particle dimension) within a few minutes of mixing. A more convenient, and certainly less unpleasant solvent than CS_2 is diethylether. In a typical preparation (ref. 2), $NaAuCl_4$ (20 mg) is dissolved in distilled water (100 ml) and treated with 2 ml of a saturated solution of yellow phosphorous in diethylether. Reduction of chloroaurate is rapid and quantitative, as demonstrated by absorption spectroscopy; and the concentration of the final solution is 5×10^{-4} mol dm^{-3}. The ruby colouration arises from an absorption peak centred at 522 nm which is thought to be attributable to a plasmon transition. (It is of interest to note in passing - and Kerker has amplified (ref. 3) this point - that Faraday also developed a method of building up films similar to those later associated with the work of Blodgett (ref. 4). A gold film, formed on the surface of a solution of auric chloride by reduction with phosphorous vapour, is capable (refs. 1 and 2) of being floated off in water and of being picked up as multilayers on a glass plate).

Though he never speculated upon their size, Faraday believed that the particles of his colloidal gold were of dimensions smaller than the wavelength of visible light. It is possible to estimate their size by ultracentrifugation and by electron microscopy. Rinde (ref. 5) concluded, on the basis of the former technique, that colloidal gold prepared according to Faraday's recipe possessed an average diamter of 19 Å. On the other hand, Turkevich and coworkers (ref. 6) concluded from low-resolution electron microscopy that Faraday's ruby coloured gold colloids had particles of average diameter 60 ± 20 Å. Using high-resolution electron microscopy, my colleagues and I have shown (ref. 7) that colloidal dispersions of gold, prepared according to Faraday's method, contain a wide distribution of particle sizes, some being as small as 30 Å others as large as 300 Å in diameter; and many of the particles occur as rather flat plates with some evidence of crystallographic twinning.

The shape of colloidal particles of gold depends markedly upon their method of preparation, as the work of Turkevich *et al* (ref. 6) clearly reveals. Reduction with boiling citric acid yields predominantly pyramidal particles, whereas hot sodium nitrate favours the production of spherical particles. Reduction with carbon monoxide, on the other hand, yields elongated cylinders whereas acetylene produces irregularly-shaped, flat plates. As was recognized in the early years of photography (ref. 8), the precise shape of colloidal particles exerts a profound influence upon the optical properties of the suspension.

Faraday's extensive studies of colloidal gold had many facets, one of these being the development of methods of producing ultra-stable gold gels, which he obtained simply by adding a warm aqueous solution of gelatin to a freshly prepared, ruby-coloured, colloidal gold sol, and allowing the gel to set. Faraday also notes that gold stains could be produced on fabric and on organic tissue. Nowadays, the use of colloidal gold to stain biological organs and to decorate such specimens for examination in the electron microscope is extensive. But, as early as 1856, Faraday impregnated ox gut with chloroaurate solution and subsequently exposed it to phosphorous vapour, thereby producing a deep ruby stain of metallic gold, which is not easily removed by washing. This work lead Faraday to devise methods of laying down coherent thin films of gold on glass, alluded to above. Such films presented him with experimental opportunities to evaluate the merits of the rival wave (undulating) and corpuscular theories of light. He remarked that these films "... may perhaps hope here to change one undulation into another, that problem which I have so long had in mind". Frequency-doubling crystals, and other modern techniques of up-conversion, which are so much in vogue these days, spring to mind on reading this passage in Faraday's Diary (ref. 9).

In highlighting some of the past achievements pertaining to colloidal metals one must pay tribute to the great achievements of German physical chemists at the turn of this century, in particular Ostwald, whose book on the "neglected" (i.e. colloidal) dimension, based in part, on lectures given at universities in the U.S.A., still makes rewarding reading. Rideal, too, another pioneering and surface chemist, was one of the first to take advantage of partially protected colloidal metal sols for heterogeneous catalysis (ref. 10).

THE PRESENT

There are a multiplicity of reasons why colloidal metals are currently of such interest, and Table 1 enumerates some of these. No longer is it adequate to restrict the term metal to certain elemental materials (Au, Pt etc.), because many oxides and sulphides, in the electronic sense of the term, have long been known to be metals. And this, after all, is the age when ceramic mixed oxides have been shown to be superconducting. Table 1 therefore includes some binary compounds that, depending upon composition, hover between the conducting and semi-conducting states. The magnetic oxides of iron, for example, present in single-crystal particles of colloidal dimension in certain bacteria, are not irrelevant to the main theme of our discussion.

TABLE 1. Popular topics in the science of colloidal metals

1.	Preparation of high-area materials for use as: catalysts, photocatalysts, adsorbents and sensors, ferrofluids; biological stains; decorating agents for assessing topography of surfaces; novel optical and nanotechnological devices.
2.	Structural challenges: Why are there magic numbers (13, 55, 147) of atoms in the more stable naked clusters? How may their structures be reliably determined? Why do simple theoretical (e.g. atom-atom approaches (refs. 13 and 14) cope so well with magic numbers, binding energies and the energetics of coulombic explosions? Are metallic clusters of colloidal dimension fluxional (refs. 15 and 16)?
3.	Thermodynamic consequences: How may one best capitalize on the differences in melting point, surface energy, electrode potential, ionization energy, etc., between small cluster and bulk materials (refs. 17 and 18)?
4.	Biological consequences of small particles (refs. 19 and 20).

My own interest in metals of colloidal dimension began some time ago when I realized that topographical features on the surface of graphite could be rendered visible by decoration with ultrafine particles of Au or Pt. Fig. 1 shows an optical micrograph, where the spiral features, symptomatic of emergent non-basal screw dislocations, can be seen. The gold decorants seen here have accreted to the micron size-range (refs. 21 and 22). When particles of gold decorants are ca 100 - 200 Å in diameter, their preferential accumulation at topographical irregularities of atomic and sub-atomic magnitude, can be readily investigated by low-power electron microscopy (ref. 23), and used to determine (ref. 24) the rates of oxidation of individual sheets of graphite parallel to the basal planes.

Such ultrafine metals and alloys - some more so than others - are very good catalysts for the oxidation of graphite; and striking anisotropic catalytic channelling phenomena associated with colloidal metals were discovered early on (ref. 25).

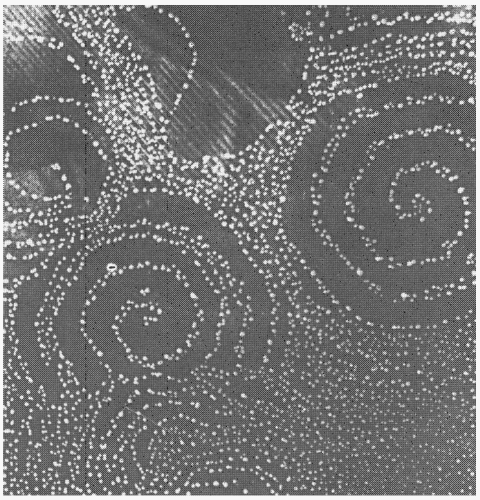

Fig. 1. Spiral features arising from the presence of emergent screw dislocations on the basal surface of graphite can be rendered visible by decoration with minute particles of gold.

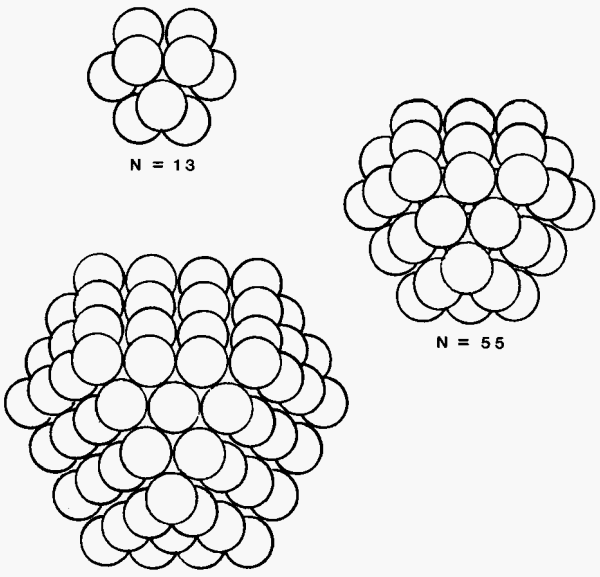

Fig. 2. Some postulated structures for assemblies of magic numbers of atoms in colloidal metals.

The decoration of the cleavage phases studied by low-power electron microscopy of minerals, such as graphite (refs. 23 and 26), molybdenite (refs. 27 and 28) and halite (refs. 29 and 30) revealed a great deal about the solid-state and surface properties of these solids, including fundamental features relating to the energetics of formation of various types of dislocation, stacking faults and point-defects, as well as epitaxy (refs. 31 and 32). With the recent arrival of scanning tunneling microscopy a great deal more can be said about both the phenomenon of epitaxy and other structural characteristics of ultrafine metals (see below).

Structural aspects

When the total number of atoms in a naked or clothed metallic colloidal particle falls between ten and a thousand, it is no easy task to determine precisely the structure of the aggregate. There is a temptation to regard as proven a structure which is no more than a plausible model. It remains to be seen, for example, whether the C_{60} 'cluster' is indeed in the form of a hollow soccer ball. And is one entitled to expect structures such as those shown schematically in Fig. 2 for the favoured atomic aggregates M_{13}, M_{55} etc., where there are the so-called 'magic numbers' of bound atoms? Somewhat surprisingly, the simplest of theoretical approaches, such as that adopted by Tomanek et al (ref. 14), yields favoured binding energies for n = 13, 55, 147 ... in the clusters M_n as well as reasonable magnitudes for other properties including the energy appropriate for coulombic explosions (i.e. the process of liberation of positively charged atoms from a multiply charged cluster M_n^{M+}). More sophisticated quantum mechanical calculations are less effective in "predicting" the magic numbers; but the more modest of such approaches (based on EHT) arrive at the important result that many configurations of clusters of the same size are very close in energy (ref. 15). In the Pt_8 cluster, for example, the cohesive enrgy of the six most active "isomers" are equal to within 0.1 eV; and for the Pt_{13} cluster very many of the configurational isomers are almost degenerate energetically.

So far as experimental studies of the structure of colloidal metals are concerned the primary methods, apart from light scattering and ultracentrifugation which yield only global size as distinct from internal structure, are as shown in Table 2.

TABLE 2. Experimental methods for probing the internal structure of colloidal metals

Radial Distribution Function (X-ray based)
X-ray Absorption Fine Structure (EXAFS)
High-resolution (Transmission) Electron Microscopy[a]
Scanning Transmission Electron Microscopy
(High-angle Rutherford Scattering)
Scanning Tunneling Microscopy (STM)

[a]In combination with X-ray Emission, Electron Energy Loss Spectroscopy and Electron Diffraction.

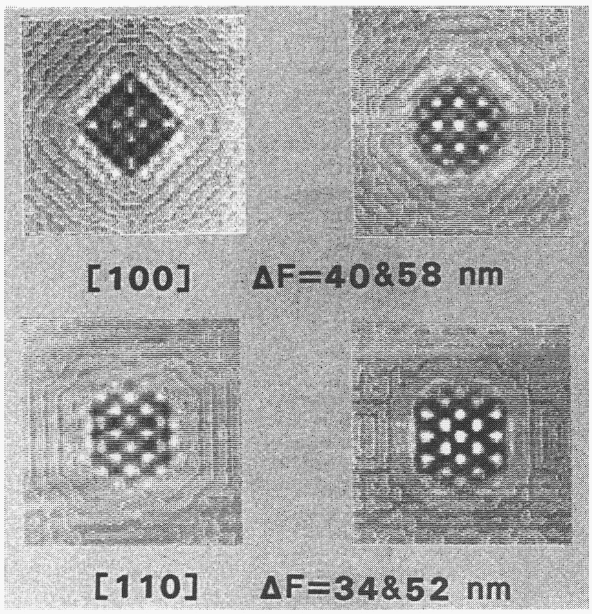

Fig. 3. Computed image for a 55 atom assembly (see Fig. 2) down two high-symmetry axes. (ΔF refers to the defect of focus for the 200 keV electron microscope JEOL 200CX)

Radial distribution functions (RDF) are invaluable for yielding M-M distances in first, second and succeeding shells, and are especially useful for charting changes in these distances when the colloidal particle is exposed to different environments. Gallezot (ref. 33) has made good use of this approach in probing the changes in bond distances when naked transition metal atom clusters (Pt, Pd, Ir...), encapsulated in zeolitic frameworks, are exposed to reactant gases such as H_2 and CO. RDF's, as is well-known from the physics of glasses and liquids, are not particularly model-sensitive, so that they do not constitute an adequate, de novo, method of determining structure.

EXAFS has proved especially valuable in studying the structure of bimetallic clusters notably by Sinfelt (ref. 11) who finds strong evidence that, in colloidal aggregates of CuRu and PtRe, the clusters, at least when supported on Al_2O_3 or SiO_2 to serve as catalysts, are not homogeneous. One or other of the pair of metals in the aggregate is preferentially exposed; correspondingly the other is preferentially bound to the support.

High-resolution electron microscopy (HREM) yields real-space, real-time images of the projected potential along particular zone axis (Fig. 3). There are ways (ref. 34) of checking the trustworthiness of images of the kind shown in Fig. 4 of a typical particle of colloidal platinum (ref. 35) and in Fig. 5 which is colloidal gold prepared according to Faraday's recipe. We have established, beyond doubt that there is indeed crystallographic order - i.e. translational symmetry - present in these minute particles of Au, Pt, Ag, Cu of colloidal dimension. Not all particles of this size are, however, crystalline, Particles of colloidal iridium dioxide - best represented as $IrO_2.xH_2O$ (ref. 36) - are deduced to be devoid of translational symmetry both from the diffuse selected-area electron diffraction patterns and high-resolution images that they yield. HREM proves unambiguously that colloidal gold prepared either according to Faraday's recipe or by other means and supported on a holey carbon film are (ref. 37) crystalline (Fig. 6).

Dynamic studies of colloidal metals have been undertaken by Iijima and Takanayagi (independently) in Japan, by Millward, Jefferson, Thomas and Brydson in the U.K. and by Bovin (Sweden) and Smith (U.S.A.). Although it is uncertain to what degree electron irradiation in the microscope sparks off the dramatic changes that are seen, it is noticable that pronounced mobility and morphological flexibility are a feature of the behaviour of these ultrafine particles of metals, as one would have expected on the basis of their thermodynamic behaviour. Takanayagi's work, from which Fig. 7 is taken, shows that the supermeshes, such as the 2 x 1 surface structure detected by LEED at Au(110), as well as the 5 x 1 supermeshes on Au(110), are very much present at the respective surfaces of the colloidal metals.

Scanning transmission electron microscopy (STEM), shortly after it was introduced in the early 1970's soon became popular as a means of identifying metallic catalysts of colloidal dimension such as Pd supported on carbon or γ-alumin by the so-called Z-contrast which entails recording (and usually ratioing) both elastic and inelastically scattered electrons. Recently Treacy and Rice (ref. 39) have devised a method of determining the sizes of minute particles even to the extent of counting the number of atoms present in the

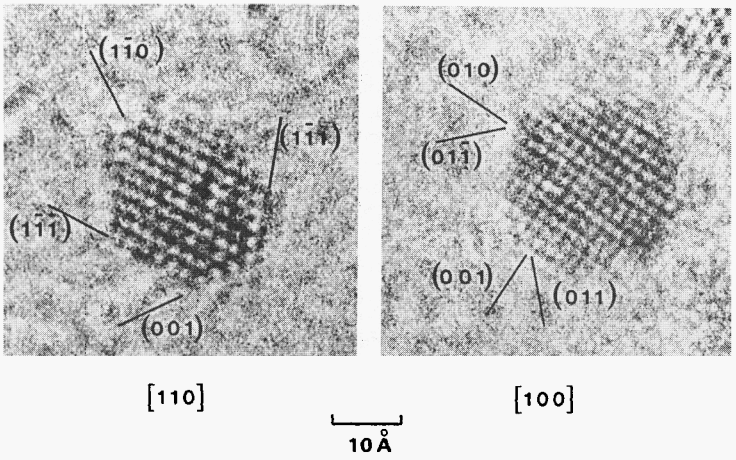

COLLOIDAL PLATINUM

Fig. 4. Typical high-resolution electron microscopic images of colloidal platinum (Millward and Thomas, unpublished work)

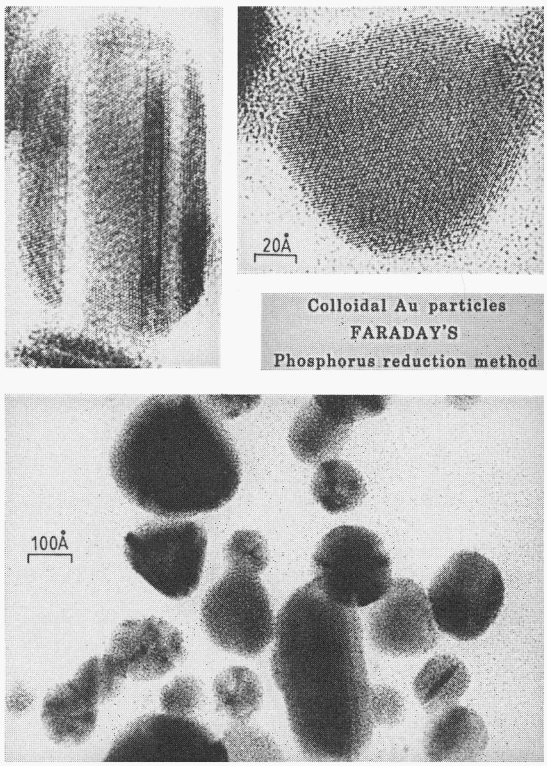

Fig. 5. High-resolution electron microscopic images of colloidal gold prepared according to Faraday's recipe. Note microtwinning visible in top left.

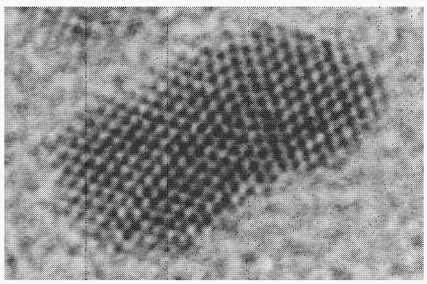

Fig. 6. Serrated edges, line defects, stacking faults with the coexistence of hexagonal close-packing and cubic-close-packing are all visible in this gold particle of colloidal dimension. Each black spot represents the projection of 5 to 8 atoms of Au.

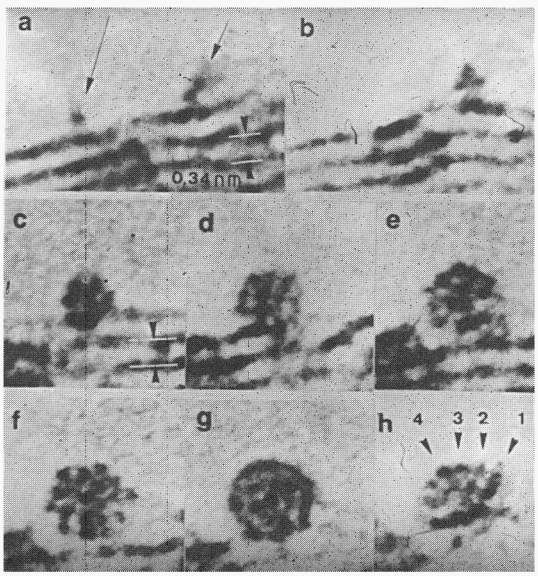

Fig. 7. A sequence of electron micrographs (taken by Dr K Takanayagi, Tokyo Inst. Technology) showing the growth of a cluster of Au of colloidal dimension on a graphite support. →

ultrafine particle. This is achieved by electron scattering into a high angle annular detector so as to avoid intensity modulations arising from Bragg reflections. The signal is mostly high-angle diffuse scattering, and is proportional to the number of atoms probed by the beam, weighted by their individual scattering cross sections. Scattering strengths of individual clusters are computed from digitized high angle annular detector images. Data for Pt on γ-Al_2O_3 (Fig. 8) when plotted as (imaged area)$^{1/2}$ *versus* (intensity)$^{1/3}$ lie close to a straight line (Fig. 9). Such plots provide calibration of the intensity increment per atom, without the necessity of external calibration. This technique has been shown (ref. 39) to be capable of detecting as few as three atoms of Pt supported on a 200 Å thick specimen of γ-Al_2O_3.

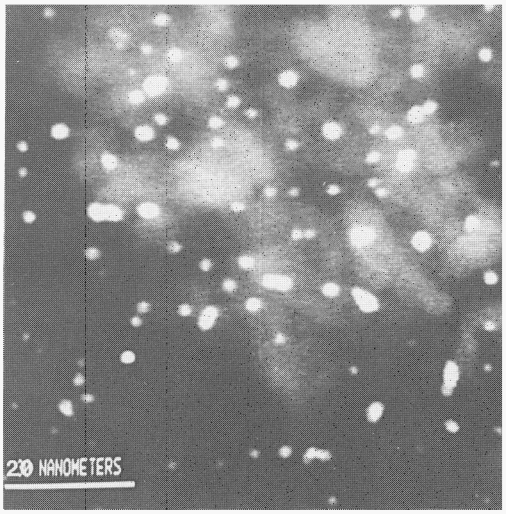

Fig. 8. Electron microscopic image of a 3 percent (wt.) of Pt supported on γ-Al_2O_3 taken with a high-angle annular detector (HAAD) in a scanning electron microscope by Treacy and Rice (ref. 39)

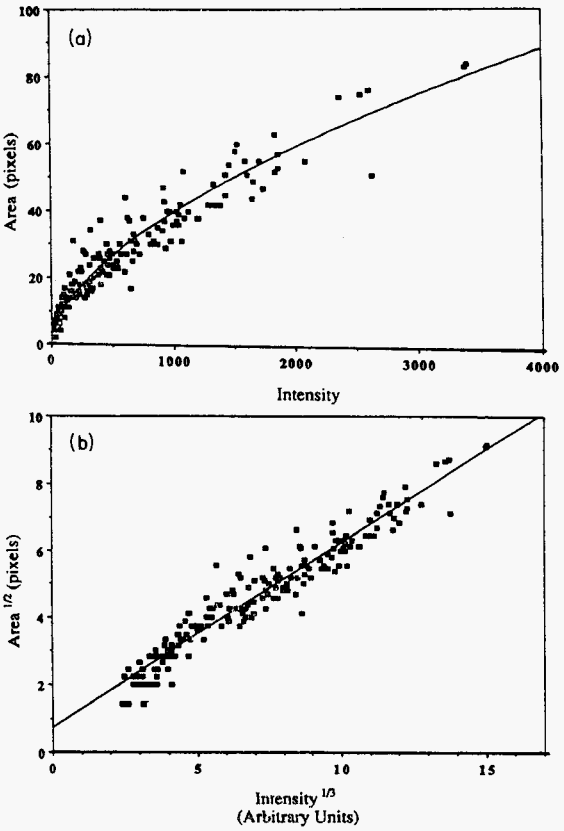

Fig. 9(a). Plot of the integrated HAAD intensity (see Fig. 8), after background subtraction, against the measured projected area for all candidate clusters visible in the image (Fig. 8)

Fig. 9(b). Intensity (I) and area (A) data from the HAAD of Fig. 9(a) plotted as $A^{1/2}$ *versus* $I^{1/3}$.

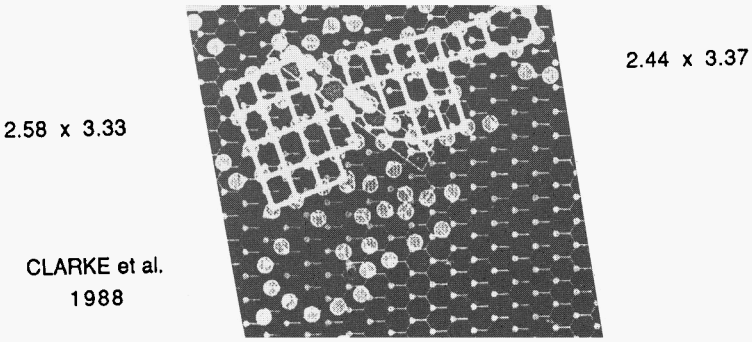

Fig. 10. Reproduction of a STM image small region (*ca* 20 x 20 Å^2) of a graphite surface on to which Ag atoms (large circles represent individual atoms of Ag) [after E. Ganz, K. Sachtler and J. Clarke, Phys. Rev. Lett, 60, 1856 (1988)].

Scanning tunneling microscopy (STM) is the newest of all the ultramicroscopic techniques (ref. 40) and one that can routinely pick out minute clusters of metals. Recent work on such clusters supported on graphite has brought to light some remarkable facts. In two-dimensional aggregates of Au or Ag grown, ostensibly epitaxially on graphite, there are both crystallographically and non-crystallographically arranged overgrowths (Fig. 10), and such arrangements vary with time. Each metal atom, initially at least, seems to occupy a unique environment. The full implications of these observations have not been fully worked out, but the role of metal-graphite interaction is thought not to be negligible. What is somewhat surprising is that rectangular lattices seem more to be preferred by the overgrowing metal, even though in three dimensions it (i.e. the Au) would take up an f.c.c. structure and the symmetry of the outermost graphitic layer is three fold about the c-axis. None of the structures of the microscopic aggregates in two dimensions seems to bear any kinship with those chronicled in the myriad metal skeletal structures of the clothed inorganic clusters.

Newer methods of preparation

Various logical extensions of the traditional methods of preparing colloidal metals have proved successful in generating alloys (ref. 13) of colloidal Pt and Au where the components seem to be distributed homogeneously within the particles: mixed aqueous solution of H_2PtCl_6 and $HAuCl_4$ when reduced with sodium nitrate solutions at 373 K yield alloy (homogeneous) sols of $Pt_{100-x}Au_x$ with size distributions of 23 ± 9 Å, 48 ± 18 Å, 143 ± 40 Å and 247 ± 64 Å when x is 0.0, 10, 50, 90 and 100.

So far as inserting colloidal Pt and other metals inside porous solids (such as zeolites) is concerned, some ingeneous methods have recently been devised. One entails the use of acetylacetonate complexes of the metal. These are reduced in situ to yield the metal in the M° state. The other, described by Sachtler et al (ref. 41) secures a higher dispersion of the transition metal cluster (e.g. colloidal Pt) inside the zeolitic cavity.

Other methods involve condensation of the highly defined (compositionally and energetically) molecular-ion beams of aggregated metals (M_n^+) such as those studied by Kaldor et al (ref. 42).

A very powerful method of producing colloidal metals dispersed in liquids is based on radiolysis with γ-rays from ^{60}Co sources. With the very high concentrations of solvated electrons an intensely reducing environment is generated. Thus ultrafine colloids of Pt and Ir (refs. 36 and 43) of mean diameter 10 to 20 Å are produced by radiolytic reduction at room temperature of the appropriate aqueous solutions. The hydrated electron, OH radicals and H_2 are the premier agents of reduction.

Why should colloidal metals be catalytically active?

The reason why the bulk metal, as distinct from the isolated atom, generally facilitates electron transfer to or from an adsorbate devolves upon the fact that the work function of the metal is much smaller than the ionization energy or electron affinity of the atom - the frontier orbitals of the metal are favourably situated energetically with respect to those of the reactants. This is a necessary but not sufficient condition. Others, notably the right coordination numbers and the right seperation distances at the catalyst surface, need to be satisfied. With small metal clusters it is possible to achieve these desiderata, for the aggregation is large enough to minimize the work function yet small enough to render available a wide range of configurational isomers (see ref. 15 and above). Moreover, because of the smallness of the particles there is maximal stabilization of the catalyst in that the majority of the atoms are exposed. Differences between one metal colloid and another arise because of a number of factors: the particular energy and symmetry of orbitals at the exposed atoms and the cohesive energy of the aggregate.

In one sense, therefore, especially when one assesses the common catalytic characteristics of colloidal metals, they may be regarded as convenient pools into, and from, which electrons may be readily transferred. In another, it is useful to recall their especial thermodynamic attributes such as electrode potentials that are significantly different from the bulk and melting points which, depending upon precise size, are markedly lower than those of the bulk material.

For both dry (e.g. gas-solid) or wet (solid-liquid) catalyzed reactions colloidal metals are likely to be superior to their bulk counterparts. This fact has been tacitly recognized from the earliest days of industrial chemistry; it is one of the reasons why supported ultrafine particles (of metals and alloys especially) are used so extensively. Dissociation (of H_2 say) and subsequent spillover onto an acidic support render processes such as the isomerization of hydrocarbons more facile.

Some specific examples

Finely divided Pt, supported on zeolites such as mordenite, are admirable isomerization catalysts and are the centrepiece of the well-known Shell 'Hysom' process. Recently (ref. 44) ultrafine particles of Pt inside a zeolite-L matrix have been shown to be

efficient catalysts for the conversion of alkanes to petrol. And colloidal metallic Ru, supported on carbon, shows exceptional promise as a catalyst for the synthesis of ammonia. With the $Pt_{100-x}Au_x$ colloidal alloys mentioned earlier interesting behaviour is observed towards hydrogenolysis and isomerization of n-butane. Whereas isomerization rates of the supported alloys (on carbon) decrease steadily with increasing content of Au, the isomerization rate passes through a maximum. Scope exists in this kind of catalyst for some fine-tuning of catalytic activity; but more work needs to be done to pin down the entire set of determinants for these processes.

Colloidal Ir is an active catalyst for reduction of water (ref. 45) and for the hydrogenation of nitrobenzene (ref. 46). We have found (ref. 36) that colloidal Ir catalyzes H_2 generation using ketyl radicals as the reducing agents. Thus u.v. radiation of compound 1, 3-(N,N,N-trimethylammonium-N-methyl) benzophenone chloride (5×10^{-4} mol dm^{-3}) in water at pH 7 containing ethanol (2 percent vol.) and colloidal Ir (1×10^{-4} mol dm^{-3}) resulted in evolution of H_2 as shown in Fig. 11.

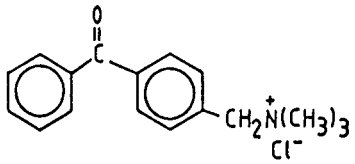

Compound 1.

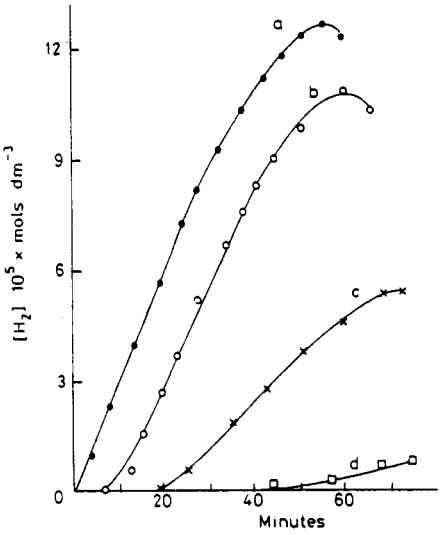

Fig. 11. Evolution of H_2 upon u.v. irradiation of the soluble benzophenone (5×10^{-4} mol dm^{-3}) at pH 7 containing ethanol (2 percent vol.) and colloidal catalysts:
(a) freshly prepared Ir,
(b) Ir colloid after exposure to air for 48 h at 40°C,
(c) Ir colloid after treating with PbO_2 and
(d) colloidal $IrO_2.xH_2O$

The initial quantum yield for formation of H_2 was 0.11, which compares well with that obtained with a Pt colloid (0.13), and the total amount of H_2 obtained (ref. 47) upon exhaustive photolysis was about 2×10^{-4} mol dm^{-3}. Assuming that all surface atoms function as active sites for colloidal Ir of diameter 15 Å, the turnover frequency for the atom is 0.03 m^{-1}. Repeating the above experiment with colloidal Ir that had been exposed to air for 48 h at 40°C also resulted in formation of H_2 (Fig. 11); but now there is a distinct induction period before H_2 evolution begins, presumably due to reduction of surface oxide by ketyl radicals. Once a clean metallic surface has been exposed, H_2 evolution takes place at the same rate as found with colloids of metallic Ir. More pronounced oxidation of the Ir surface is achieved by treatment of the colloid with PbO_2. The resulting blue colloid has an Ir core surrounded either with $IrO_2.xH_2O$ or a mixed oxide of the type PbO.IrO. This has a longer induction period.

THE FUTURE

Table 1 reminds us that colloidal metals have considerable roles to play in the future both on the fundamental scientific and applied fronts. In optics, magnetism and the world of devices much scope for exploitation exists. In the world of catalysis, especially photocatalysis, new and important opportunities have arisen in the context of harnessing solar energy. The tasks involved in encouraging the photogeneration of both oxygen and hydrogen from water have been well rehearsed (ref. 50). Less well known, perhaps, are some alternative prospects.

In recent years photochemists have recognised (ref. 48) the possibilities offered by the incorporation of colloidal catalysts into their reaction mixtures. The nature of the products can be profoundly altered by using different types of colloidal catalyst. Moreover,

there is real hope that useful products, not just H_2, but chemical building blocks, are realisable from waste products. This situation has been exemplified by Harriman (ref. 48) with reference to the photochemistry of benzophenone in aqueous alcoholic solution.

Under normal conditions, u.v. radiation of benzophenone results in quantitative population of the lowest energy excited triplet state, which is of nπ^* character, and rapidly extracts a hydrogen from the alcohol. The resulting ketyl radicals undergo addition and/or disproportunation reactions and benzpinacal is formed with high quantum yield. But when the photolysis is carried out in the presence of small amounts of colloidal Pt, benzpiracal formation if inhibited and H_2 is freely liberated (ref. 51). This occurs because intermediate ketyl radicals are powerful reducing agents and can reduce water to H_2 on the surface of the colloidal Pt. Colloidal Au and Ir function similarly (ref. 43).

Improvements can be made to the photo system by using benzophenone derivations that are more water soluble e.g. compound 1. As mentioned earlier, u.v. irradiation of 1 in water containing 4 percent ethanol results in quantitative formation of benzpinacal and acetaldehyde; but if colloidal Pt is added (2×10^{-4} mol dm^{-3}) H_2 liberation proceeds with a quantum yield of 0.34, as indicated in Scheme 1.

Scheme 1

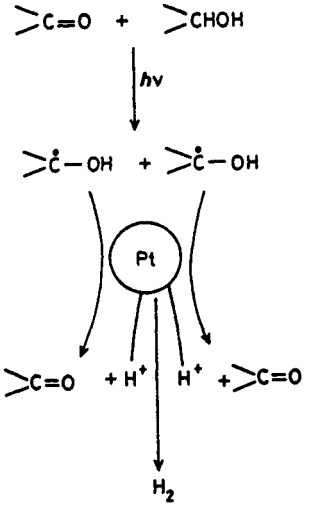

Scheme 2

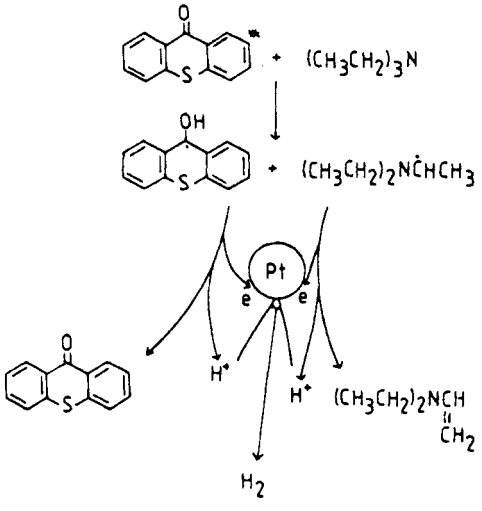

The initial reaction involves abstraction of a H atom from an ethanol molecule by the triplet excited state phenone derivative, thereby producing two ketyl radicals within a solvent cage. Those radicals that escape from the solvent cage are capable of recombination and addition reactions but these processes are in competition with electron transfer to a colloidal particle of Pt, which functions as a microelectrode and accepts an electron from each ketyl radical. This oxidizes the ketyl radical to the corresponding carbonyl compound (hence recycling the benzophenone) and stores electrons on the colloid. Discharge of H_2 entails the reduction of surface bound protons followed by recombination. The overall reaction ($C_2H_5OH \longrightarrow CH_3CHO + H_2$) stores some 42 kJ mol^{-1}.

Though extremely simple, and versatile in its adaptability, this photochemical reaction operates with only a low sunlight conversion efficiency (ca 1.7 percent). Numerous other donors (in place of ethanol) could be used, sacrificially, with the benzophenone to yield H_2. Thus the quantum efficiency for H_2 production from triethylamine is close to unity and for ethylamine to a half. The principles outlined here of choosing the right photosensitizer (in this case a benzophenone), donor and colloidal catalyst offers considerable scope for improvement. Thus Harriman et al (ref. 50) in these Laboratories, using a slightly different system and pursuing the same general principles, arrived at an effective photocatalytic method of generating H_2 [with sacrificial consumption of triethylamine (see Scheme 2)].

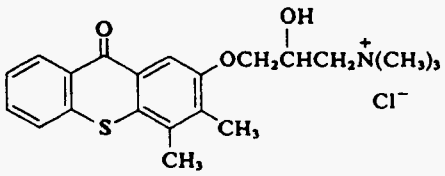

Compound 2.

Irradiation of a water-soluble 9-oxothioxanthene (2) at 400 nm in the presence of triethylamine and colloidal Pt produced H_2 with an optimized quantum yield of H_2 obtained upon exhaustive photolysis (0.08 mol dm^{-3}) is superior to all other reported systems. The fraction of the solar system harvested by 2 is still unacceptably low for commercial exploitation; but this can be improved by simple synthesis. Harriman draws attention to the many other donors (sulphides, ureas and phenols as well numerous industrial waste products) that could replace the amine as donor.

As well as modifying the sensitizers and the donors in photo-stimulated reactions, we may well enquire what scope have we to play tunes with the metal? A great deal. Let us first recall that, in order to ensure high rates of liberation of H_2, it is necessary to use high concentrations of catalyst, an end best achieved by employing colloidally dispersed material. But producing small particles is not the only means of ensuring that the catalyst thwarts the self-annihilation of the reducing radicals. And, by the same arguments, having small particles does not guarantee that trapping will be effective. Other factors, notably electrostatic forces and radical mobility have to be considered. A clothed (protected) colloidal particle will carry a surface charge due to ionisable groups; and the magnitude and sign of this change will, in general, vary with pH and on the presence of other surface adsorbed species. (The whole question of ease of interfacial electron-transfer reactions between colloidal Pt and reducing radicals derived from various aryl ketones, N-methylpyridinium ions etc. - as listed in Fig. 12 - has been examined recently by Harriman et al (ref. 52). The rate of electron transfer is not controlled solely by the available surface area).

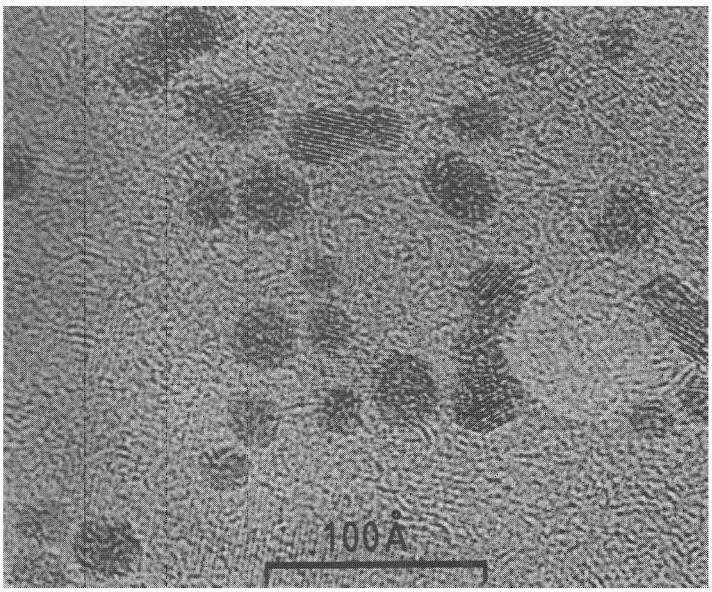

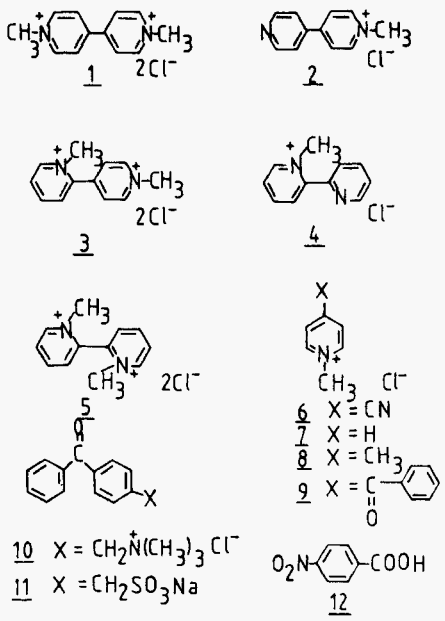

Fig. 12. The structural formulae of the electron mediators (source of reducing radicals) used by Harriman et al (ref. 52) to study interfacial electron-transfer reactions at the surfaces of colloidal platinum, shown left.

Colloids of other metals, besides Pt, can be readily prepared (Au, Ag, Tl, Ir, Ru, Ni, Cu and Pd). Under the same conditions of preparation, colloids of Pt and Ir tend to give much smaller particle sizes (ca 7 to 10 Å diameter) than those of Ag (30 to 40 Å diameter) which in turn are smaller than those of Au (60 to 70 Å). H_2 liberation is greatly facilitated at colloidal Pt and Ir because of their low intrinsic overpotentials. But with colloids of Ag, which have high overpotentials, many more electrons can be stored at the particle surface before H_2 liberation takes place. Colloids of Cd and Tl are even more reluctant to liberate H_2 so that many hundreds of electrons can be stored at the surface of each colloidal particle. Upon addition of suitable substrates, these electrons can be discharged and used to drive multielectron reductions.

We conclude, therefore, by recalling that the prospect of reducing CO_2 (on, say, Ru colloids) and nitrate ions to ammonia (on Ag colloids) decomposing chlorinated hydrocarbons (on Tl colloids) are real; and it is by no means impossible that an appropriate colloidal metal or alloy system can be devised for reduction of N_2 to ammonia. Furthermore, by a combination of photo-assisted dehydrogenation and the addition of readily available simple reactants, quite novel syntheses should be possible. The scheme below is, in principle, a feasible route to amino-acid production in the presence of colloidal Pt.

Scheme 3

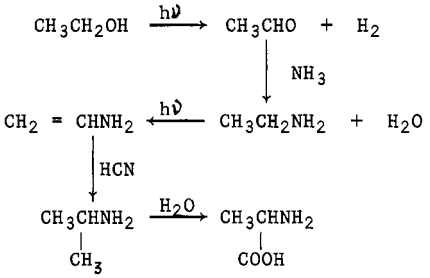

Acknowledgements

I thank the S.E.R.C. for support and Drs. A. Harriman, M-C. Richoux, G.R. Millward and M.M.J. Treacy for many stimulating discussions.

REFERENCES

1. M. Faraday, Phil. Trans. Roy. Soc. 147, 145 (1857).
2. A. Harriman, M-C. Richoux and J.M. Thomas, in preparation.
3. M. Kerker, J. Coll. Interf. Sci. 112, 302 (1986).
4. K.B. Blodgett, J. Amer.Chem. Soc. 57, 1007 (1935).
5. E. Rinde in The Distribution of Sizes of Colloidal Gold Sols Prepared According to the Nuclear Method, Uppsala (1928).
6. J. Turkevich, P.C. Stevenson and J. Hillier, Disc. Faraday Soc. 11, 55 (1951).
7. D.A. Jefferson, J.M. Thomas, G.R. Millward, K. Tsuno, A. Harriman and R.D. Brydson, Nature 323, 428 (1986).
8. R. Gans, Am. Phys. Leipzig 37, 881 (1912); 47, 270 (1915).
9. Faraday's Diary VII, Bell and Sons, London (1935).
10. E.K. Rideal, J. Amer. Chem. Soc. 42, 749 (1920).
11. J.H. Sinfelt, Bimetallic Catalyst, Wiley, New York (1983).
12. P.A. Sermon, J.M. Thomas, K. Keryou and G.R. Millward, Angewandte Chemie, Intl. Ed., 26, 918 (1987).
13. G. Natanson, F. Amar and R.S. Berry, J. Chem. Phys. 78, 399 (1983).
14. D. Tomanek, S. Mukherjee and K.H. Bennemann, Phys. Rev. B 28, 665 (1983).
15. M. Simonetta, Nouveau J. de Chemie 10, 533 (1986).
16. B. Bigot and C. Minot, J. Amer. Chem. Soc. 106, 6602 (1984).
17. The whole issue of Surface Science 106 (1981).
18. Metal Clusters (ed. F. Frager and G. zu Putlitz), Springer-Verlag, New York (1986).
19. R.B. Frankel, Nature 320, 575 (1986).
20. S. Mann, T.T. Moensch and R.J.P. Williams, Proc. Roy. Soc. 221, 38 (1984); see also S. Mann, Nature 332, 119 (1988).
21. J.M. Thomas, Chemistry and Physics of Carbon (ed. P.L. Walker, jr) 1, p.122 (M. Dekker, 1965).
22. J.M. Thomas and C. Roscoe, ibid 3, 1 (M. Dekker, 1968).
23. J.M. Thomas, E.L. Evans and J.O. Williams, Proc. Roy. Soc. 331, 417 (1972).
24. E.L. Evans, R.J.M. Griffiths and J.M. Thomas, Science 171 174 (1971).
25. J.M. Thomas and P.L. Walker, jr, J. Chem. Phys. 41, 587 (1964).
26. G.R. Hennig, Chemistry and Physics of Carbon (ed. P.L. Walker, jr) 2, p.1 (M. Dekker, 1966).

27. O.P. Bahl, E.L. Evans and J.M. Thomas, Surface Science 8, 473 (1967).
28. E.L. Evans and J.M. Thomas, Trans. Faraday Soc. 64, 3354 (1968).
29. H. Betghe, R. Scholtz and V. Schmidt, Disc. Faraday Soc. 38, 79 (1964).
30. G.A. Bassett, D.W. Menter and D.W. Pashley, Proc. Roy. Soc. A246, 345 (1958).
31. D.W. Pashley, Advanc. Phys. 14, 327 (1965).
32. E.L. Evans and J.M. Thomas, Carbon 5, 586 (1967).
33. P. Gallezot, Catalysis Sci. and Tech. 5, 221 (1984).
34. J.M. Thomas, Ultramicroscopy 8, 11 (1982).
35. G.R. Millward and J.M. Thomas, unpublished work.
36. A. Harriman, G.R. Millward and J.M. Thomas, New J. of Chemistry 11, 757 (1987).
37. G.R. Millward, A. Harriman and J.M. Thomas, unpublished work.
38. M.M.J. Treacy, A. Howie and C.J. Wilson, Phil. Mag. A38, 569 (1978).
39. M.M.J. Treacy and S.B. Rice, to be submitted.
40. G. Binnig and H. Rohrer, Surface Science 126, 236 (1983).
41. W.H.M. Sachtler, M.S. Tzau and H.J. Jiang, Solid State Ionics 26, 71 (1988).
42. A. Kaldor, D.M. Cox, D.J. Trevor and M.R. Zakin, ref. 18, p195.
43. A. Henglein, Modern Trends in Colloid Science and Chemistry and Biology (ed. H.F. Bicke) Birkhauser Verlag, Stuttgart, p126 (1985).
44. J.R. Bernard, Proc. Fifth Intl. Conf. on Zeolites (ed. L.V.C. Rees), p686, Hayden, London (1980).
45. G. Mills and A. Henglein, Radiat. Phys. Chem. 26, 391 (1985).
46. J. Belloni, M.O. Delcourt and C. Lectere, Nouv. J. Chem. 6, 507 (1982).
47. A. Harriman, J. Chem. Soc. Faraday Trans. 2 82, 2267 (1986).
48. A. Harriman, Plat. Metals Rev. 31, 125 (1987).
49. J. Davila, A. Harriman and M-C. Richoux, J. Chem. Soc. Faraday Trans 2 84, 287 (1988).
50. M. Kirch, J.M. Lehn and J.P. Sauvage, Helv. Chim. Acta 62, 1345 (1979).
51. C.K. Gratzel and M. Gratzel, J. Amer. Chem. Soc., 101, 7741 (1979).
52. A. Harriman, G.R. Millward, P. Neta, M-C. Richoux and J.M. Thomas, J. Phys. Chem. 92, 1286 (1988).